

THERMODYNAMIC AND KINETIC PARAMETERS OF THE PROCESSES OF DEUTERIUM INTERACTION WITH TUNGSTEN PROTECTIVE COATINGS[†]

 **Sergiy Karpov**,  **Valeryi Ruzhytskyi**,  **Galyna Tolstolutskaya***,  **Ruslan Vasilenko**,
 **Oleksandr Kuprin**,  **Sergiy Leonov**

National Science Center "Kharkov Institute of Physics and Technology", Kharkov, Ukraine

**Corresponding Author: g.d.t@kipt.kharkov.ua*

Received September 30, 2021; revised October 22, 2021; accepted November 18, 2021

The effect of radiation damage on the retention of deuterium in tungsten (W) was examined. A vacuum-arc plasma source with magnetic stabilization of the cathode spot was used for tungsten coatings preparation. W samples were treated with D ions at temperatures 300-600 K with a fluence of $(1 - 10) \cdot 10^{20} \text{ D}_2^+/\text{m}^2$ and ion energies of 12 keV/D₂⁺. The influence of radiation damage on microstructure and accumulation of deuterium implanted in W samples at room temperature and after annealing have been studied. Thermal desorption (TD) spectroscopy was used to determine the D retained throughout the bulk of the sample. The structure of TD spectra represents the multi-stage process of deuterium release suggesting the trapping of gas atoms by a number of defect types. Computational evaluation of deuterium desorption within the framework of the diffusion-trapping model allows to associate characteristics of experimental TD spectra with specific trapping sites in the material. Experimental TD spectrum was fitted by assigning four binding energies of 0.55 eV, 0.74 eV, 1.09 eV and 1.60 eV for the peaks with maxima at 475, 590, 810 and 1140 K, respectively. The low temperature peak in the TD spectra is associated with desorption of deuterium bounded to the low energy natural traps, whereas the other peaks are related to the desorption of deuterium bounded to the high energy ion induced traps: monovacancies and vacancy clusters.

Keywords: tungsten, irradiation, damage, microstructure, thermal desorption, deuterium trapping, activation energies, de-trapping processes

PACS: 52.40HF, 28.52FA, 68.49SF, 79.20RF

An important problem in the development of fusion plasma devices that utilize tritium is the loss of tritium from the fuel cycle. The tritium leaking can cause safety issues because of the regulatory limits for the amount of tritium in the vessel walls. In addition, operational problems due to possible uncontrolled hydrogen isotopes recycling fluxes can affect global plasma stability. It is therefore advisable to investigate the features of the thermal release of hydrogen isotopes from plasma-facing materials in order to evaluate their applicability as candidate materials with respect to fuel retention [1].

Currently, tungsten is selected as the main armor material for the plasma-facing components of the next step fusion reactor due to a high melting point, low tritium retention, low sputtering ratio as well as good behavior under neutron irradiation. A lot of works has been performed to qualify existing materials related to issues for fusion reactor ITER, in particular for W, as plasma facing materials for first wall and diverter [2]. However, it is now believed that fabrication the first wall of a fusion reactor completely from tungsten is not economically feasible due to the high cost, as well as the difficulties with machining due to the hardness and brittleness of tungsten. Recently, tungsten coatings on a stainless steel substrate have come to be considered as an alternative option from the point of view of economics and protection of structural material against plasma exposure [3]. In order to evaluate the applicability of W-coatings as plasma-facing materials, it is necessary to carefully examine the behavior of these materials under intense neutron irradiation from the fusion reaction and plasma exposure. Understanding the mechanisms of microstructural changes during operation is also of high importance.

Extensive studies have been made on the interaction of hydrogen isotopes with various tungsten materials [1–10]. The surface topography of W bulk prepared by powder sintering (20 μm thickness), and W coatings deposited by cathodic arc evaporation and by argon ion sputtering was studied under the influence of low-energy hydrogen (deuterium) and helium plasma at room temperature [4, 5]. The exposure predominantly resulted in the formation of blisters and sputtering. After helium and deuterium plasma irradiation, numerous blisters were observed on the surface of W foils samples and coatings deposited by argon ion sputtering. The surface of W coatings deposited by cathodic arc evaporation was undergone only sputtering process under the same irradiation conditions [4]. Processes of sputtering, surface modification and deuterium retention in W coatings deposited on stainless steel by cathodic arc evaporation were studied under the influence of low-energy (500 eV) deuterium plasma with a fluence of $4 \cdot 10^{24} \text{ D}^+/\text{m}^2$ at room temperature. The values of the experimentally measured sputtering yield of the tungsten coatings exposed to the D plasma are two times higher compared to bulk W but almost an order of magnitude smaller compared to ferritic martensitic steels. The total D retentions of W coatings were on the order of $5 \cdot 10^{19} \text{ D}/\text{m}^2$ [5].

Since the solubility of hydrogen isotopes in tungsten is very low, the trapping at defects mainly determines the retention. These defects are either natural defects which are present after fabrication or they may be created by treatment

[†] *Cite as:* S. Karpov, V. Ruzhytskyi, G. Tolstolutskaya, R. Vasilenko, O. Kuprin, and S. Leonov, East. Eur. J. Phys. **4**, 99 (2021), <https://doi.org/10.26565/2312-4334-2021-4-11>

© S.Karpov, V.Ruzhytskyi, G.Tolstolutskaya, R.Vasilenko, O.Kuprin, S. Leonov, 2021

after fabrication such as, for example, radiation-induced defects. Therefore, parameters of trapping are essential for predicting hydrogen isotope transport in irradiated tungsten. Many aspects of hydrogen retention in bulk tungsten have been investigated in the past and the available literature is extensive [6-10]. However, there are few data on the behavior of hydrogen isotopes in tungsten coatings.

The objective of this study is to evaluate the role of radiation defects on deuterium retention in tungsten coatings prepared by cathodic arc evaporation (CAE) and irradiated with energetic deuterium ions.

MATERIAL AND METHODS

Tungsten coatings were deposited on tungsten substrates by means of PVD method using unfiltered cathodic arc evaporation in a “Bulat-6” system equipped with a W (99.9%) cathode of 60 mm diameter. Magnetic stabilization of the cathode spot was used in a vacuum-arc plasma source [11]. The main advantage of the cathodic arc evaporation method over conventional magnetron sputtering deposition is a much higher degree of plasma ionization and energy of metallic ions [12]. This can be the explanation of the high quality and adhesion of such deposited coatings.

Tungsten foil was chosen as a substrate material to eliminate the possible influence of various effects from other substrate materials, for example, differences in thermal expansion coefficients, mutual diffusion of elements, eutectic formation, etc., during high-temperature annealing in TD experiments. This approach in choosing W foils as substrates was used to study the TD of deuterium [13, 14], helium blistering [15], TD of helium [16], as well as in determining the thermal stability [17] of the W coatings deposited by magnetron sputtering.

The tungsten foil substrates (8×5×0.3 mm) were chemically degreased and ultrasonically cleaned in a hot alkaline bath for 10 min and dried in warm air. After cleaning they were mounted on a substrate holder without rotation. The substrate-cathode distance was about 250 mm. The chamber was evacuated to a pressure of 2×10^{-3} Pa before the coating deposition. The substrates were ion etched with tungsten ion bombardment by applying a DC bias of -1300 V during 3 min. The arc current was 120 A. Noble gas Ar (99.9 %) was introduced in to vacuum chamber up to pressure of 2 Pa for stabilization of the arc discharge. The deposition of tungsten coating was performed at a substrate bias voltage of -30 V and a substrate temperature of ~ 400 °C. The deposition time was 60 min. The coating thickness was ~ 8 μm. The concentration of impurities ions (oxygen, nitrogen and carbon) did not exceed 3 at.% in accordance with the EDX and WDS data.

Hydrogen isotopes trapping by irradiation damages is often simulated using higher energy ion irradiation technique to introduce the defects, such as dislocation loops, vacancies and voids, etc [9]. In the current study, W foils and coatings have been irradiated with deuterium ions at temperatures 300 - 600 K with a fluence of $(1 - 10) \cdot 10^{20}$ D₂⁺/m² and ion energies of 12 keV/D₂⁺. The SRIM code [18] was used to evaluate the ion projected ranges (R_p) and range straggling (ΔR_p), the concentration of gas atoms, and the dpa (displacement per atom) (Fig. 1). The calculations were performed with a target density of 19.35 g cm⁻³ and a displacement threshold energy of 90 eV [9].

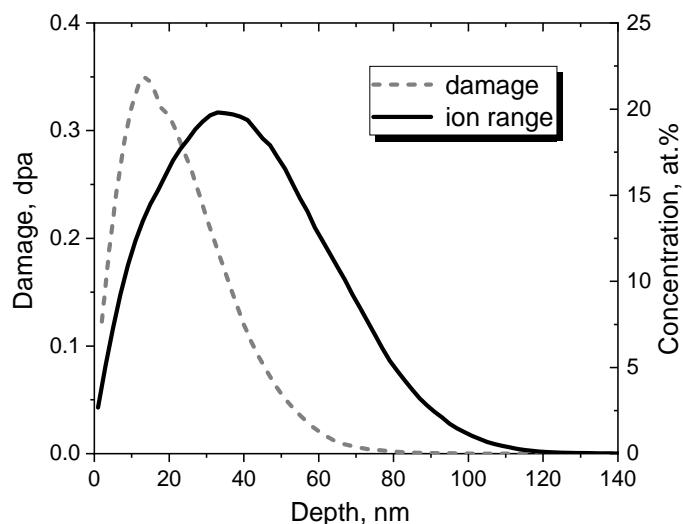


Figure1. Depth distribution profiles of damage and concentration for 12 keV/D₂⁺ in tungsten calculated for a fluence of $1 \cdot 10^{21}$ m⁻²

The specimen temperature was measured by the thermocouple and was maintained at about (27 ± 2.5) °C during irradiation. The experimental ion flux and fluence were calculated from the measured ion currents and beam spot areas. The deuterium release from irradiated specimens was investigated by the thermal desorption technique in the temperature range from 300 to 1400 K at a rate of 6 K s⁻¹. This temperature range is expected to encompass the characteristic detrapping temperatures of hydrogen isotopes with radiation defects in tungsten materials [6]. The gas release was registered by a monopole mass-spectrometer. Irradiations and measurements of TD spectra were performed in one chamber, to exclude contact of the specimens with air that prevented the formation of artifact trap sites associated with the surface. The residual gas pressure in the experimental chamber was measured to be $\sim 5 \cdot 10^{-5}$ Pa.

The microstructure of tungsten substrate and coatings was investigated using transmission electron microscopy at room temperature, employing standard bright-field techniques on JEM-2100 electron microscope. Investigations of surface microstructure were performed using scanning electron microscope JEOL JSM-7001F. Chemical composition of the coatings was determined by energy dispersive X-ray spectroscopy – EDS.

RESULTS AND DISCUSSION

Fig. 2 shows SEM images of surface morphology, cross-section images and TEM microstructure of tungsten foil substrates and W coatings deposited by CAE in the initial state.

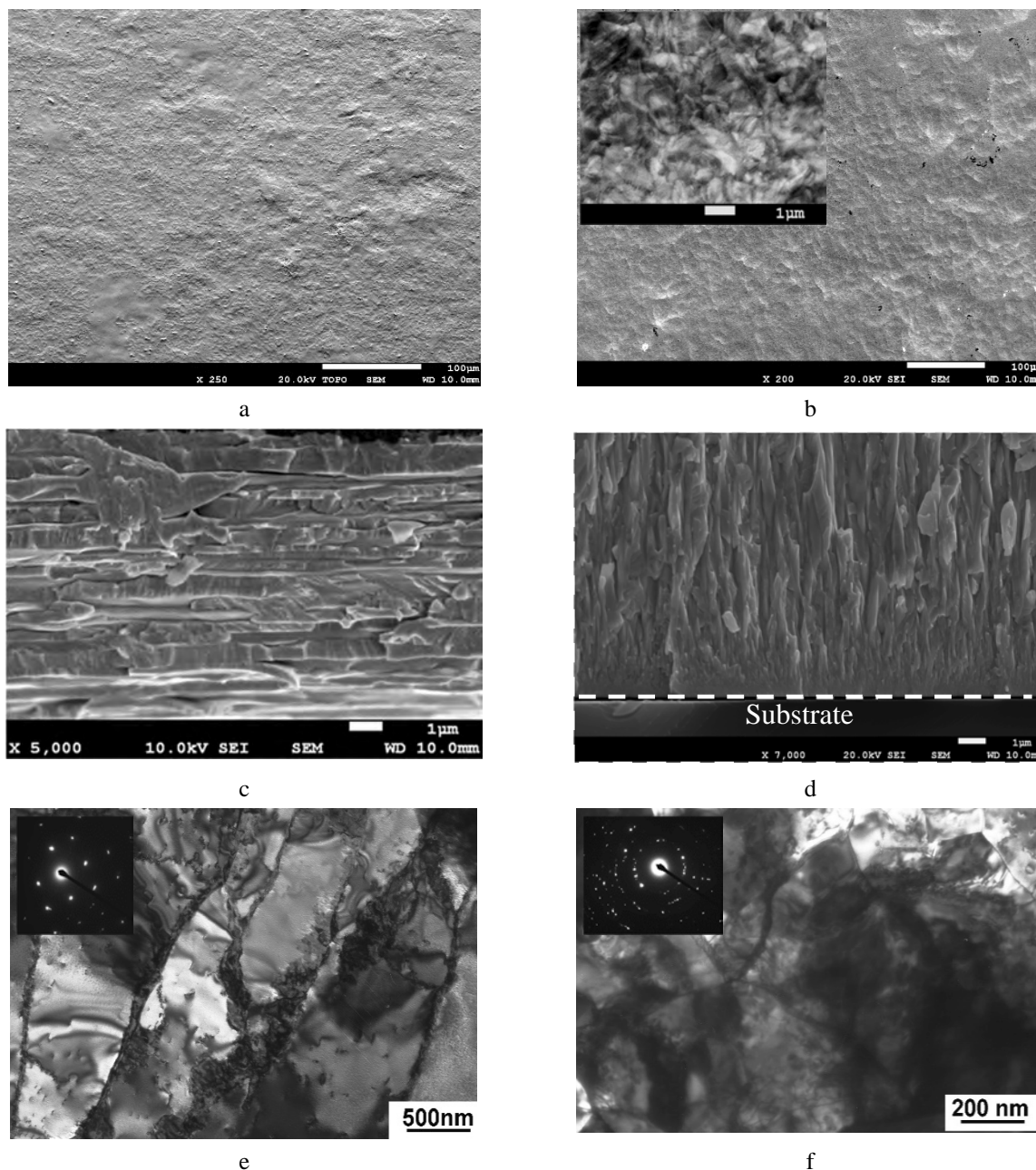


Figure 2. Structure of tungsten foil (a,c,e) and coating (b,d,f): SEM surface morphology (a,b) and cross-section (c,d); TEM plan view (e,f). Higher magnification detail of the ‘nanoridges’ coating morphology (insert fig. 2, b). The interface between the coating and substrate is indicated by the dashed horizontal line (Fig. 2, d).

Surface morphology of tungsten foil substrates has ‘smoothing’ relief (Fig. 2a). The microstructure of the tungsten foil substrates was characterized by layers with high elongation grains arranged parallel to the surface, see Fig. 2c. TEM investigation demonstrated high elongation grains with dimensions in the 0.5-1.5 μm range. Dislocations were distributed inhomogeneously even within a single grain (Fig. 2e). The dislocation density was found to be about $1 \cdot 10^{14} \text{ m}^{-2}$. The dislocation density was measured by counting the number of intersections with dislocation lines made by random strips drawn on micrographs.

The as-deposited W coatings have a rough surface (Fig. 2b). Surface morphology of initial W coatings exhibit surfaces of densely packed “nanoridges” or overlapping tiles, which is the typical morphology of refractory metal films deposited at the relatively low temperatures (see Fig. 2b, insert). These “nanoridges” were observed on the α -W phase film surfaces irrespective of the film thickness. It is found that many individual grains contain two types of “nanoridge” domains oriented with each other with an angle ranging between 109 and 124°. Each domain has ridges with an average height and period of (1.5 ± 0.5) and (7.5 ± 1.0) nm, respectively [4]. As-deposited W coating show a typical columnar epitaxial growth with grain boundaries preferentially oriented perpendicular to the substrate (Fig. 2d). The structure of W-coating is dense and without pores, as shown on SEM cross-section image (Fig. 2d).

According to the TEM analysis data, a single α -W phase with an average grain size of 180 nm is formed in the tungsten coatings. The density of dislocations was found to be about $2.2\cdot 10^{14} \text{ m}^{-2}$. The structure of coatings may be explained by sufficiently high relative energy of tungsten ions (140 eV) and by the high degree of plasma ionization (90 %) of the tungsten cathodic arc [12, 19].

Figs. 3-4 shows deuterium TD spectra from tungsten substrates and coatings irradiated with deuterium ions at temperature 300 K with a fluence of $(2-10)\cdot 10^{20} \text{ D}_2^+/\text{m}^2$ and ion energy of 12 keV/D₂⁺.

Gas evolution from both types of specimens is characterized by the following common features: (i) initial temperature of desorption is consistent with the terminal temperature of exposure; (ii) the structure of TD spectrum represents the multi-stage process with well-defined desorption peaks at about 600, 850 and 1150 K for all studied irradiation fluences with the exception of high-temperature desorption stage for smallest fluences; (iii) the broad low temperature desorption stage looks like a peak with shoulders, and thus appears to consist of several narrow peaks.

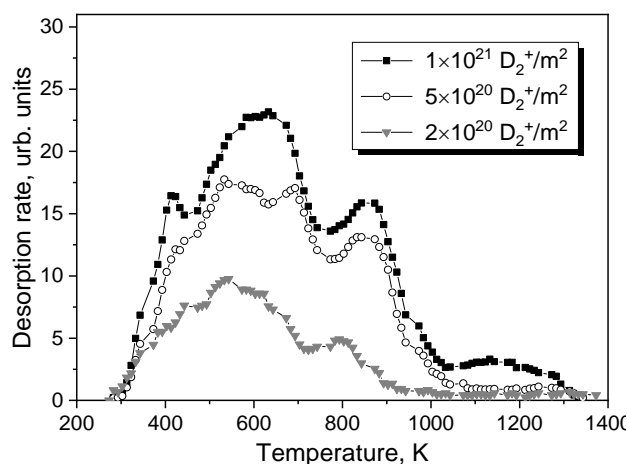


Figure 3. Deuterium TD spectra from tungsten foils after deuterium ions irradiation at temperature 300 K

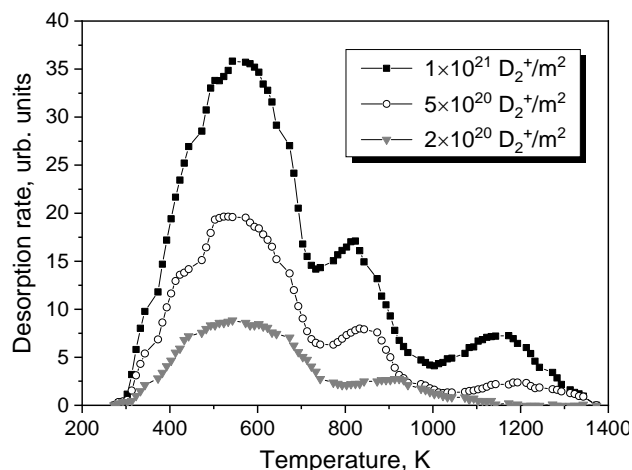


Figure 4. Deuterium TD spectra from tungsten coatings after deuterium ions irradiation at temperature 300 K

Characteristic temperatures of TD spectra depend on hydrogen retention parameters, predominantly on activation energy of de-trapping processes. In the case of the keV implantation, both radiation-induced and natural trap types are present in the material.

Energetic ion irradiation can greatly increase the local point defects concentration by displacing the lattice atoms through collisions. The 6 keV D⁺ energy is well above the threshold for displacement damage [20] and capable of creating Frenkel pair defects within the implantation zone. At room temperature, the interstitials are mobile [21] and most of them quickly recombine with vacancies, however a fraction of vacancies survives and becomes the dominant deuterium traps in near surface layer of material. On the other hand, several studies [6,7] of the damage structure produced in W crystals under D ion implantation have revealed that in addition to radiation-induced defects, intrinsic defects strongly influence deuterium retention. Moreover, intrinsic defects like dislocations and grain boundaries are thought to be responsible for accumulation of large amounts of deuterium, especially in polycrystalline W at near room temperatures.

The deuterium concentration is found to be inhomogeneous throughout the bulk, according to previously published data on the evolution of the deuterium depth distribution as a function of fluence [22, 23]. The highest deuterium content is observed in the ion stopping range, while a decreasing tail of deuterium concentration with reaching the plateau is detected at depths of up to several microns. It has been shown, that the near surface high concentration layer is associated with radiation-induced defects, whereas the latter zone is related to natural defects in the material, since certain portion of the D atoms implanted in tungsten at room temperature diffuse deep into the bulk and is captured by dislocations and grain boundaries.

Computational evaluation of deuterium desorption within the framework of the diffusion-trapping model [24] provides the ability to assess activation energies of de-trapping processes and to associate characteristics of experimental TD spectra with specific trapping sites in the material. This was accomplished by numerically solving the equations for diffusion in a field of traps.

$$\frac{\partial C(x,t)}{\partial t} = D(T) \frac{\partial^2 C(x,t)}{\partial x^2} - \sum_k \frac{\partial G_k(x,t)}{\partial t} + \phi(x) \quad (1)$$

$$\frac{\partial G_k(x,t)}{\partial t} = 4\pi R_k D(T) \left\{ C(x,t) [W_k(x,t) - G_k(x,t) / m_k] - G_k(x,t) z N_V \exp\left(-\frac{Q_k}{k_B T}\right) \right\},$$

where C is the concentration of hydrogen in the solution; G_k is the concentration of hydrogen in traps of k -type; R_k is the radius of defect trap; m_k is the number of hydrogen atoms per trap; z is the number of solution sites per host atom; N_V is the atomic density of the host; W_k is trap concentration; $\phi(x)$ is the distribution of the hydrogen introduction rate through depth; Q_k is the binding energy of hydrogen atom with the trap; k_B is Boltzmann's constant; and $D(T) = D_0 \exp(-E_m/k_B T)$ is the deuterium diffusivity.

Since solute deuterium atoms remain mobile in tungsten at room temperature, the calculations include two steps imitating the experimental procedure: deuterium implantation at room temperature, and then linear heating of the sample to the certain temperature.

Present calculations assumed up to four different trap energies. This assumption is supported by the thermal desorption data (see Fig. 4) that show at least three clearly visible peaks, and by preliminary estimations indicating the complex structure of low temperature desorption stage, which is not a simple single peak, but rather composed of several narrower peaks that suggest the presence of multiple trap energies.

Model calculations also assumed that injected deuterium diffuses through the material, interacting with intrinsic and radiation defects. The defect traps representing radiation-induced displacement defects are distributed along the depth according to the damage profile calculated using SRIM (see Fig. 1) and located in the near-surface region within 100 nm of the surface. Obviously, natural defects are distributed over the whole thickness of the sample, but in present calculations they were assumed to distribute uniformly in the depth range of 0-2 microns. Both these assumptions are supported by the results [25, 26] of experimentally measured depth distribution of keV-energy deuterium in tungsten after implantation at 300 K.

Modeling of thermal desorption data suggest a rate-dependent boundary conditions, that requires the value for the recombination coefficient. The obtained values for the hydrogen recombination coefficient on tungsten vary by more than six orders of magnitude [27-29]. Current calculations utilize recently published data [30] for experimentally measured recombination coefficient for a pristine and clean W surface under well-controlled surface conditions by means of X-ray photoelectron spectroscopy. We used the coefficient $K_r = 3.8 \times 10^{-26} \exp(-0.15/kT) \text{ m}^4 \text{ s}^{-1}$ for the pristine surface due to special preparation of specimens' surface was not performed.

Other necessary calculation parameters include $N_V = 6,3 \cdot 10^{28} \text{ m}^{-3}$, $D = 2.9 \times 10^{-7} \exp(-0.39/kT) \text{ m}^2 \text{ s}^{-1}$ [31]; $R_k = 3,16 \cdot 10^{-10} \text{ m}$; $z = 6$.

The system of equations (1) was solved numerically by previously described and used method [24, 32]. The best agreement between the calculated and experimental deuterium TD spectrum is shown in Fig. 5.

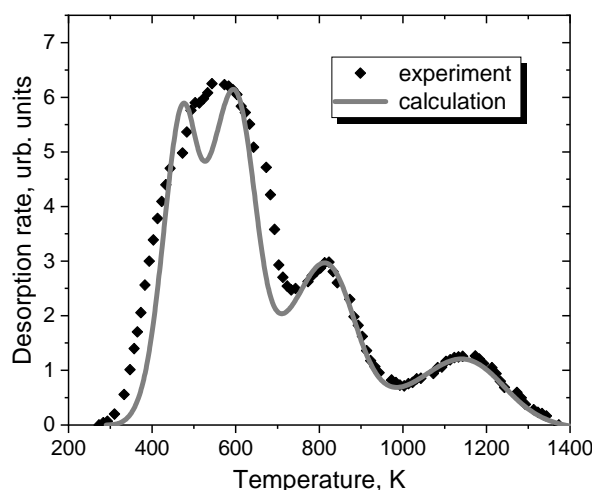


Figure 5. Experimental points and the calculated curve of thermal desorption of deuterium from W coating irradiated at temperature 300 K by 12 keV D_2^+ ions to a fluence of $1 \cdot 10^{21} \text{ m}^{-2}$

Experimental TD spectrum is rather well fitted by assigning four binding energies of 0.55 eV, 0.74 eV, 1.09 eV and 1.60 eV for the peaks with maxima at 475, 590, 810 and 1140 K, respectively. The corresponding trapping energies representing binding energies plus the activation energy for diffusion (0.39 eV [31]) are 0.94 eV, 1.13 eV, 1.48 eV and 1.99 eV. The first peak in the TD spectra appears to be associated with desorption of deuterium bounded to the low energy natural traps, whereas the other peaks are related to desorption of deuterium bounded to the high energy ion induced traps.

The low-temperature desorption peak with binding energy of 0.5-0.6 eV is often attributed to natural defects without separation of trap types into impurities, dislocations, grain boundaries, etc. In present study high dislocation density has

been observed in the microstructure of W coatings (Fig. 2) that suggests the dominative role of dislocation type defects on the formation of 475 K low-temperature peak. In addition, the derived binding energy value of 0.55 eV for this peak correlates well with results of ab initio atomistic calculations [33] demonstrating that hydrogen atoms in tungsten are bound to the screw dislocation core with the binding energy of ~ 0.6 eV.

Hydrogen isotope retention in various W grades has been studied quite extensively under different experimental conditions. Under low-energy irradiation, vacancies are considered to be the predominant radiation-induced defects. The value of hydrogen de-trapping energy from a single vacancy in W varies among different researchers in the range of 1.3-1.6 eV [34-36]. Therefore, it appears reasonable to suppose that the desorption peak with a de-trapping energy of 1.48 eV in our spectrum can be interpreted as the deuterium release from monovacancies.

Recent ab-initio calculations have demonstrated that multiple hydrogen atoms can be trapped around a single defect, leading to a distribution of binding energies [36-38]. Furthermore, trapping of multiple hydrogen atoms in one monovacancy is quite possible and the binding energy of subsequent H atoms decreases with increasing occupancy. Following density functional theory calculations [36-37, 39], hydrogen capturing with de-trapping energy in the range of 1.1-1.2 eV can be attributed to hydrogen multiplicity binding in monovacancies, where it is energetically favorable for up to six hydrogen atoms to participate in the occupancy. Based on these findings, desorption stage with a maximum at 590 K and characterized in our simulations by de-trapping energy of 1.13 eV is associated with deuterium release from multiply occupied monovacancies.

The ion-irradiated tungsten coatings also showed deuterium desorption in the high-temperature region, i.e. 1000-1300 K. The high temperature peak is usually associated with deuterium trapped in vacancy clusters [23, 40-42]. The de-trapping energy of 1.99 eV attributed to this peak in our calculations correlates with previously published values of hydrogen de-trapping energy from vacancy cluster – in the range of 1.7–2.2 eV [23, 34-35, 43-44]. It is worth noting, that this desorption stage is absent at lowest implantation fluence (see Fig. 4) due apparently to impeded vacancy clustering caused by the deficiency of monovacancies.

Fig. 6 shows deuterium TD spectra for tungsten coating after deuterium ions irradiation to a fluence of $1 \cdot 10^{21} \text{ D}_2^+/\text{m}^2$ at different temperatures T_{room} – 600 K. The D retention is strongly reduced at high implantation temperatures of 500-600 K compared to that at 300 K. These observations agree with [45] where it was shown the deuterium retention of Plansee tungsten decreased at irradiation with energy upon 200 eV/D^+ and increasing irradiation temperature in the 300-500 K range. The highest retention level was $\sim 1.7 \cdot 10^{20} \text{ D}^+/\text{m}^2$ at 300 K, followed by a linear decreasing trend, reaching $\sim 5 \cdot 10^{19} \text{ D}^+/\text{m}^2$ at 500 K [45].

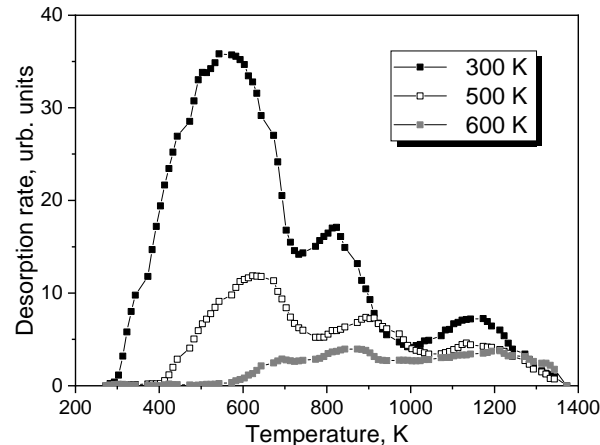


Figure 6. Deuterium TD spectra from tungsten coatings after deuterium ions irradiation to a fluence of $1 \cdot 10^{21} \text{ D}_2^+/\text{m}^2$ at different temperatures 300 – 600 K

The desorption stage associated with natural defects is characterized by a noticeable gas release already at ~ 400 K and a maximum at about 475 K. Therefore, the amount of trapped deuterium in low-energy intrinsic traps decreases rapidly at implantation temperature of 500 K, whereas the population in the stronger radiation-induced traps varies slightly at this temperature. High-energy traps population begin to decrease considerably after 600 K as the sample temperature is high enough for de-trapping of deuterium from those traps.

CONCLUSIONS

In the present study, deuterium interaction with tungsten protective coatings deposited by cathodic arc evaporation has been investigated by means of ion irradiation combined with thermal desorption spectroscopy. Scanning and transmission electron microscopy were used for specimen's microstructure characterization. W samples were treated with D ions at temperatures 300 - 600 K with a fluence of $(1 - 10) \cdot 10^{20} \text{ D}_2^+/\text{m}^2$ and ion energies of 12 keV/D_2^+ . Characteristics of experimental TD spectra were associated with specific trapping sites in the material on the base of computational evaluation of deuterium desorption within the framework of the diffusion-trapping model. The main results are summarized as follows.

Deuterium gas release from tungsten coatings and tungsten foils demonstrates similar trend.

The trapping of ion-implanted deuterium in tungsten is attributed to the interaction of gas atoms with natural and radiation-induced defects.







The trapping energies of deuterium with traps are determined within the framework of the diffusion-trapping model. The derived trapping energy values of 0.94 eV, 1.13 eV, 1.48 eV and 1.99 eV are associated with deuterium interaction with intrinsic dislocations, radiation-induced monovacancies at multiple and single deuterium occupation, and vacancy clusters, respectively.

It was found that an increasing of the implantation temperature leads to a significant decrease of deuterium retention in tungsten coatings.

Acknowledgements

The work was financially supported by the National Academy of Science of Ukraine (program “Support of the development of main lines of scientific investigations” (KPKVK 6541230)).

ORCID IDs

 **Sergiy Karpov**, <https://orcid.org/0000-0002-6607-8455>;
  **Valeriy Ruzhytskyi**, <https://orcid.org/0000-0002-7856-1188>
 **Galyna Tolstolutska**, <https://orcid.org/0000-0003-3091-4033>;
  **Ruslan Vasilenko**, <https://orcid.org/0000-0002-4029-9727>
 **Oleksandr Kuprin**, <https://orcid.org/0000-0003-4293-4197>;
  **Sergiy Leonov**, <https://orcid.org/0000-0002-0338-9168>

REFERENCES

- [1] M.A. Abdou, E.L. Vold, C.Y. Gung, M.Z. Youssef, and K. Shin, *Fusion Technology*, **9**, 250 (1986), <https://doi.org/10.13182/FST86-A24715>
- [2] R.A. Pitts, X. Bonnin, F. Escourbiac, H. Frerichs, J.P. Gunn, T. Hirai, A.S. Kukushkin, E. Kaveeva, M.A. Miller, D. Moulton, V. Rozhansky, I. Senichenkov, E. Sytova, O. Schmitz, P.C. Stangeby, G. De Temmerman, I. Veselova, and S. Wiesen, *Nucl. Mater. Energy*, **20**, 100696 (2019), <https://doi.org/10.1016/j.nme.2019.100696>
- [3] C. Ruset, E. Grigore, H. Maier, R. Neu, H. Greuner, M. Mayer, and G. Matthews, *Fusion Eng. Des.*, **86**(9-11), 1677 (2011), <https://doi.org/10.1016/j.fusengdes.2011.04.031>
- [4] A.V. Nikitin, A.S. Kuprin, G.D. Tolstolutska, R.L. Vasilenko, V.D. Ovcharenko, and V.N. Voyevodin, *PAST*, **2**(114), 29 (2018), https://vant.kipt.kharkov.ua/ARTICLE/VANT_2018_2/article_2018_2_29.pdf
- [5] G.D. Tolstolutska, A.S. Kuprin, A.V. Nikitin, I.E. Kopanets, V.N. Voyevodin, I.V. Kolodiy, R.L. Vasilenko, A.V. Ilchenko, *PAST*, **2**(126), 54 (2020), https://vant.kipt.kharkov.ua/ARTICLE/VANT_2020_2/article_2020_2_54.pdf
- [6] V.Kh. Alimov, J. Roth, *Phys. Scr.* **2007**, 6 (2007), <https://doi.org/10.1088/0031-8949/2007/T128/002>
- [7] O.V. Ogorodnikova, J. Roth, and M. Mayer, *J. Appl. Phys.* **103**, 034902 (2008), <https://doi.org/10.1063/1.2828139>
- [8] J. Roth, K. Schmid, *Phys. Scr.* **2011**, 014031 (2011), <https://doi.org/10.1088/0031-8949/2011/T145/014031>
- [9] M. Kobayashi, M. Shimada, Y. Hatano, T. Oda, B. Merrill, Y. Oya, and K. Okuno, *Fus. Eng. Des.* **88**, 1749 (2013), <https://doi.org/10.1016/j.fusengdes.2013.04.009>
- [10] A. Manhard, K. Schmid, M. Balden, and W. Jacob, *J. Nucl. Mater.* **415**, S632 (2011), <https://doi.org/10.1016/j.jnucmat.2010.10.045>
- [11] A.S. Kuprin, S.A. Leonov, V.D. Ovcharenko, E.N. Reshetnyak, V.A. Belous, R.L. Vasilenko, G.N. Tolmachova, V.I. Kovalenko, and I.O. Klimenko, *PAST*, **5**(123), 154 (2019), https://vant.kipt.kharkov.ua/ARTICLE/VANT_2019_5/article_2019_5_154.pdf
- [12] A. Anders, *Surf. Coat. Technol.* **257**, 308 (2014), <https://doi.org/10.1016/j.surfcoat.2014.08.043>
- [13] P. Wang, W. Jacob, L. Gao, S. Elgeti, and M. Balden, *Phys. Scr.* **T159**, 014046 (2014), <https://doi.org/10.1088/0031-8949/2014/T159/014046>
- [14] P. Wang, W. Jacob, and S. Elgeti, *J. Nucl. Mater.* **456**, 192 (2015), <http://doi.org/10.1016/j.jnucmat.2014.09.023>
- [15] J. Yu, W. Han, Z. Chen, and K. Zhu, *Nucl. Mater. Energy*, **12**, 588 (2017), <http://doi.org/10.1016/j.nme.2016.10.001>
- [16] J. Yan, X. Li, Z. Wang, and K. Zhu, *Nucl. Mater. Energy*, **22**, 100733, (2020), <https://doi.org/10.1016/j.nme.2020.100733>
- [17] N. Gordillo, C. Gómez de Castro, E. Tejado, J.Y. Pastor, G. Balabanian, M. Panizo-Laiz, R. Gonzalez-Arrabal, J.M. Perlado, and J. del Rio, *Surf. Coat. Technol.* **325**, 588 (2017), <http://dx.doi.org/10.1016/j.surfcoat.2017.06.070>
- [18] R.E. Stoller, M.B. Toloczko, G.S. Was, A.G. Certain, S. Dwaraknath, and F.A. Garner, *Nucl. Instrum. Methods Phys. Res. Sect. B: Beam Interact. Mater. Atoms*, **310**, 75 (2013), <http://dx.doi.org/10.1016/j.nimb.2013.05.008>
- [19] I.I. Aksenov, A.A. Andreev, V.A. Belous, V.E. Strel'nitskij, and V.M. Khoroshikh, *Vacuum arc: plasma sources, deposition of coatings, surface modification*, (Naukova Dumka, Kyiv, 2012).
- [20] W. Eckstein, *Springer Series in Materials Science, vol. 10*, (Springer, Berlin, 1991), <https://doi.org/10.1007/978-3-642-73513-4>
- [21] P. Jung, *Atomic Defects in Metals, Landolt-Bornstein New Series III/25*, edited by H. Ullmaier, (Springer, Berlin, 1991)
- [22] V. Kh. Alimov, J. Roth, and M. Mayer, *J. Nucl. Mater.* **337-339**, 619 (2005), <http://dx.doi.org/10.1016/j.jnucmat.2004.10.082>
- [23] O.V. Ogorodnikova, J. Roth, and M. Mayer, *J. Appl. Phys.* **103**, 034902, (2008), <https://doi.org/10.1063/1.2828139>
- [24] S.O. Karpov, V.V. Ruzhits'ky, I.M. Neklyudov, V.I. Bendikov, and G.D. Tolstolutska, *Metallofiz. Noveishie Tekhnol.* **26**, 1661 (2004).
- [25] V. Kh. Alimov, K. Ertl, J. Roth, and K. Schmid, *Phys. Scr.* **T94**, 34 (2001), <https://doi.org/10.1238/Physica.Topical.094a00034>
- [26] T. Ahlgren, K. Heinola, K. Vörtler, and J. Keinonen, *J. Nucl. Mater.* **427**, 152 (2012), <https://doi.org/10.1016/j.jnucmat.2012.04.031>
- [27] R.A. Anderl, D.F. Holland, G.R. Longhurst, R.J. Pawelko, C.L. Trybus, and C.H. Sellers, *Fusion Tech.* **21**, 745 (1992), <https://doi.org/10.13182/FST92-A29837>
- [28] C. Garcia-Rosales, P. Franzen, H. Plank, J. Roth, and E. Gauthier, *J. Nucl. Mater.* **233-237**, 803 (1996), [https://doi.org/10.1016/S0022-3115\(96\)00185-7](https://doi.org/10.1016/S0022-3115(96)00185-7)
- [29] P. Franzen, C. Garcia-Rosales, H. Plank, and V.Kh. Alimov, *J. Nucl. Mater.* **241-243**, 1082, (1997), [https://doi.org/10.1016/S0022-3115\(97\)80198-5](https://doi.org/10.1016/S0022-3115(97)80198-5)
- [30] M. Zhao, S. Yamazaki, T. Wada, A. Koike, F. Sun, N. Ashikawa, Y. Someya, T. Mieno, and Y. Oya, *Fusion Eng. Des.* **160**, 111853 (2020), <https://doi.org/10.1016/j.fusengdes.2020.111853>

- [31] R. Frauenfelder, J. Vac. Sci. Technol. **6**, 388 (1969), <https://doi.org/10.1116/1.1492699>
- [32] G.D. Tolstolutskaaya, V.V. Ruzhytskyi, V.N. Voyevodin, I.E. Kopanets, S.A. Karpov, and A.V. Nikitin, J. Nucl. Mater. **442**(1-3), S710 (2013), <https://doi.org/10.1016/j.jnucmat.2013.02.053>
- [33] D. Terentyev, V. Dubinko, A. Bakaev, Y. Zayachuk, W.V. Renterghem, and P. Grigorev, Nucl. Fusion, **54**, 042004 (2014), <https://doi.org/10.1088/0029-5515/54/4/042004>
- [34] H. Eleveld, and A. van Veen, J. Nucl. Mater. **191-194**(Part A), 433 (1992), [https://doi.org/10.1016/s0022-3115\(09\)80082-2](https://doi.org/10.1016/s0022-3115(09)80082-2)
- [35] M. Poon, A.A. Haasz, and J.W. Davis, J. Nucl. Mater. **374**, 390 (2008), <https://doi.org/10.1016/j.jnucmat.2007.09.028>
- [36] K. Heinola, T. Ahlgren, and K. Nordlund, J. Keinonen, Phys. Rev. B, **82**, 094102 (2010), <https://doi.org/10.1103/PhysRevB.82.094102>
- [37] N. Fernandez, Y. Ferro, and D. Kato, Acta Mater. **94**, 307 (2015), <https://doi.org/10.1016/j.actamat.2015.04.052>
- [38] K. Ohsawa, J. Goto, M. Yamakami, M. Yamaguchi, and M. Yagi, Phys. Rev. B, **82**, 184117 (2010), <https://doi.org/10.1103/PhysRevB.82.184117>
- [39] Y.-W. You, X.-B. Wu, Y.-C. Xu, Q.F. Fang, J.L. Chen, G.-N. Luo, C.S. Liu, B.C. Pan, and Z. Wang, AIP Adv. **3**, 012118 (2013), <https://doi.org/10.1063/1.4789547>
- [40] M. Fukumoto, H. Kashiwagi, Y. Ohtsuka, Y. Ueda, M. Taniguchi, T. Inoue, K. Sakamoto, J. Yagyu, T. Arai, I. Takagi, and T. Kawamura, J. Nucl. Mater. **390-391**, 572 (2009), <https://doi.org/10.1016/j.jnucmat.2009.01.107>
- [41] I.I. Arkhipov, S.L. Kanashenko, V.M. Sharapov, R.Kh. Zalavutdinov, and A.E. Gorodetsky, J. Nucl. Mater. **363-365**, 1168 (2007), <https://doi.org/10.1016/j.jnucmat.2007.01.150>
- [42] Yu. Gasparyan, M. Rasinski, M. Mayer, A. Pisarev, and J. Roth, J. Nucl. Mater. **417**, 540 (2011), <https://doi.org/10.1016/j.jnucmat.2010.12.119>
- [43] A. van Veen, H.A. Filius, J. de Vries, K.R. Nijkerk, G.J. Rozing, and D. Segers, J. Nucl. Mater. **155-157**, 1113 (1988), [https://doi.org/10.1016/0022-3115\(88\)90478-3](https://doi.org/10.1016/0022-3115(88)90478-3)
- [44] Yu.M. Gasparyan, O.V. Ogorodnikova, V.S. Efimov, A. Mednikov, E.D. Marenkov, A.A. Pisarev, S. Markelj, and I. Čadež, J. Nucl. Mater. **463**, 1013 (2015), <https://doi.org/10.1016/j.jnucmat.2014.11.022>
- [45] Z. Tian, J.W. Davis, and A.A. Haasz, J. Nucl. Mater. **399**, 101 (2010), <https://doi.org/10.1016/j.jnucmat.2010.01.007>

ТЕРМОДИНАМІЧНІ ТА КІНЕТИЧНІ ПАРАМЕТРИ ПРОЦЕСІВ ВЗАЄМОДІЇ ДЕЙТЕРІЮ ІЗ ЗАХИСНИМИ ПОКРИТТЯМИ ВОЛЬФРАМУ

Сергій Карпов, Валерій Ружицький, Галина Толстолуцька, Руслан Василенко, Олександр Купрін, Сергій Леонов
Національний науковий центр "Харківський фізико-технічний інститут", Харків, Україна

Досліджено вплив радіаційних пошкоджень на утримання D в вольфрамі (W). Для приготування вольфрамових покриттів використовувалося вакуумно-дугове плазмове джерело з магнітною стабілізацією катодної плями. Зразки W опромінювали іонами D при температурах 300-600 K до дози (1-10) 10^{20} D₂⁺/м² з енергією іонів 12 кеВ / D₂⁺. Досліджено вплив радіаційних пошкоджень на мікроструктуру і накопичення дейтерію, імплантованого в зразки W при кімнатній температурі і після відпалу. Термодесорбційна спектроскопія (ТДС) використовувалася для визначення D, утримуваного в об'ємі зразків. Структура ТД-спектра являє собою багатоступінчастий процес виділення дейтерію, який свідчить про захоплення атомів газу дефектами кількох типів. Розрахункова оцінка десорбції дейтерію в рамках моделі дифузійного захоплення дозволила зв'язати характеристики експериментальних ТД-спектрів з конкретними центрами захоплення в матеріалі. Експериментальний ТД-спектр досить добре апроксимується шляхом присвоєння чотирьох енергій зв'язку 0,55 еВ, 0,74 еВ, 1,09 еВ і 1,60 еВ для піків з максимумами при 475, 590, 810 і 1140 K, відповідно. Низькотемпературний пік в спектрах ТД, вірогідно, пов'язаний з десорбцією дейтерію, асоційованого з природними пастками з низькою енергією зв'язку, тоді як інші піки пов'язані з десорбцією дейтерію з пасток, індукованих іонами високої енергії: моновакансій та вакансійних кластерів.

Ключові слова: вольфрам, опромінення, пошкодження, мікроструктура, термодесорбція, уловлювання дейтерію, енергія активації